energies

MDPI

Article

Impact of Increased Travel Speed of a Transportation Set on the Dynamic Parameters of a Mine Suspended Monorail

Kamil Szewerda [1,*], Jarosław Tokarczyk [1] and Andrzej Wieczorek [2]

[1] KOMAG Institute of Mining Technology, Pszczyńska 37 Street, 44-100 Gliwice, Poland; jtokarczyk@komag.eu
[2] Faculty of Mining, Safety Engineering and Industrial Automation, Silesian University of Technology, Akademicka 2 Street, 44-100 Gliwice, Poland; andrzej.n.wieczorek@polsl.pl
* Correspondence: kszewerda@komag.eu

Abstract: The method of increasing the efficiency of using one of the most common means of auxiliary transport in underground coal mines—suspended monorails—is presented. Increase of velocity is one of the key parameters to improve the efficiency and economical effect related with the underground auxiliary transport. On the other hand, increasing the velocity results in bigger value of force acting on the suspended monorail route and its suspensions. The most important issue during increasing the velocity is ensuring the required safety for the passengers and not overloading the infrastructure. In order to analyze how increasing velocity influences the level of loads of the route suspension and the steel arch loads, the computational model of suspended monorail was developed. The computational model included both the physical part (embedded in the program environment based on the Multi-Body System method) and the components of the monorail control system. Two independent software environments were cooperating with each other through the so-called co-simulation. This model was validated on the base of results obtained on the test stand. Then, the numerical simulations of emergency braking with different values of velocity were conducted, which was not possible with the use of physical objects. The presented study can be used by the suspended monorail's producers during the designing process, and leads to increase the safety on underground transportation routes.

Keywords: mining transport; suspended monorail; stand test; multi-body system; numerical calculation; coal mines

Citation: Szewerda, K.; Tokarczyk, J.; Wieczorek, A. Impact of Increased Travel Speed of a Transportation Set on the Dynamic Parameters of a Mine Suspended Monorail. *Energies* **2021**, *14*, 1528. https://doi.org/10.3390/en14061528

Academic Editor: Nikolaos Koukouzas

Received: 15 February 2021
Accepted: 8 March 2021
Published: 10 March 2021

1. Introduction

Suspended monorails are one of the basic auxiliary transportation means in underground mining plants. The design of the monorails allows the transportation of materials as well as the personnel. The design of the monorails is constantly developed to improve both transportation possibilities, safety [1–3], and at the same time, the distances between the shaft and the mining face are being extended, both as a result of the expansion of mining fields and as a result of organizational changes. As the length of the routes increases, the time the personnel spends commuting to the workplace also increases. The popularity of suspended monorails is due to many advantages, including: High lifting capacity and efficiency; the possibility of using long, branched routes; possibility of avoiding obstacles on the floor, and easy reloading of floor mounted railways. Moreover, in suspended monorails, the route is isolated from the floor, which, in certain geological and mining conditions, may uplift and deform [4–6].

The maximum permissible speed of a suspended monorail during the people movement depends on the country and the applicable law, and is 1–3.3 m/s. In some European countries, preparatory work to introduce legislative changes increasing the maximum permissible speed of suspended monorails during personnel movement has been underway in recent years [7–9]. Both manufacturers of suspended monorails, who improve their machines, and mining plants that use this type of transportation are interested in increasing this speed limit. The main benefit of increasing the speed of monorails is the extension of the effective working time of the personnel, which translates into measurable economic benefits and an increase in the profitability of the coal mining process.

Of course, for safety reasons, the speed limit will be increased on the route sections that are properly prepared and tested. Ensuring the load to a single roof support arch below 40 kN (in a certain case, a load of 50 kN is allowed with the consent of the mining plant operation manager, providing the results of the calculations) is one of the criteria the route must meet that the suspended monorail can move along it.

Contrary to railways, where the rails are stationary and integrated with the ground, there are extensive and detailed methods of identifying vibrations of the running components [10]. In suspended monorails the route is assembled, lifted, and stabilized by means of slings, which changes the flow of forces between the means of transport and its surroundings. Increasing the speed is possible with maintain the existing level of safety.

Determining the forces in slings with the use of analytical methods is difficult due to the fact that the suspended line is a system that is statically indeterminate. Therefore, the numerical MBS method was used.

As the weight of the suspended monorail used for the crew movement is much lower than the mass of the assembly dedicated to the transportation of heavy materials (e.g., powered roof supports or longwall shearer components), exceeding the maximum permissible load to the roof support arches is unlikely. However, three aspects should be taken into account in the context of increasing the maximum permissible speed of the monorail moving the personnel. The first one is the fact that the dynamic overloads in emergency situations, such as emergency braking, are greater than the loads resulting from static calculations. Second, increasing the travel speed will result in an exponential increase in kinetic energy and side-sway amplitude [11]. This energy must be dissipated during the emergency braking process. In connection with the above, it is necessary to verify the level of dynamic overloads in the suspensions of the suspended monorail route, which directly affect the yielding roof support [7,12–15]. The results of the authors' analyses of loads to the suspensions of the suspended monorail's route in terms of the possibility of increasing the permissible speed of the monorail while moving the personnel is presented. Based on the emergency braking tests carried out on the test track, it was possible to validate the suspended monorail calculation model. This model was used in numerical simulations to assess the impact of changing the speed of a suspended monorail on the load to the route suspensions.

2. Test Stand and Computational Model

Test stand was built at the premises of one of the manufacturers of suspended monorails. The stand uses an innovative type of 4 m long rails to stabilize the route and increase the personnel's comfort during travel. The rails design is the result of implementation of the European INESI project [7]. The length of the entire route on the test track was 90 m. Figure 1 shows the test stand.

Figure 1. View of the test stand [2].

Each rail joint at the test stand was connected to a traverse, suspended from the stand frame with two chains. Successive pairs of chains were alternately installed vertically (perpendicular to the longitudinal axis of the rail) or they were deflected, forming the shape of the letter "V" (Figure 2).

Figure 2. Method of rail suspension: Straight suspensions (**left**); V-shaped suspensions (**right**) [7].

Fourteen force transducers were fitted to the selected suspensions to record the tensile force in the suspension during the monorail travel or braking. The sensors were designed in such a way to replace three chain links in the suspension (Figure 3).

Figure 3. Force transducers installed in the rail suspensions [7].

The suspended monorail was accelerated to the set speed with which it was moving along the test track, and at the end of the test track, the transportation set stopped. The second option was accelerating the transportation set and then initiating emergency braking at a selected point on the route. Apart from the tensile forces acting in the suspensions, the speed and acceleration of the monorail were recorded during the tests.

A computational model of the suspended monorail, consisting of two parts: the dynamic part and the dynamic part control module, was developed at the later stage.

Recreation of the suspended monorail with the route on the test stand is the dynamic part of the computational model. The dynamic part of the computational model was built using the software analyzing the kinematics and dynamics of multi-body systems. This part of the model is shown in Figure 4.

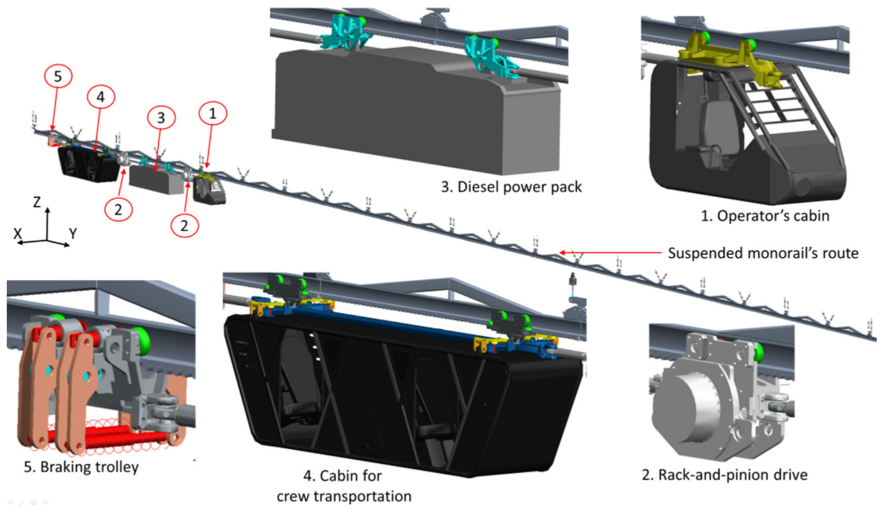

Figure 4. Computational model of a suspended monorail on the test stand [7].

Computational model consists of:

- 383 rigid bodies:
  - Operator's cabin (7 rigid bodies);
  - 2x rack-and-pinion drive (2x 6 rigid bodies);
  - diesel power pack (11 rigid bodies);
  - cabin for crew transportation (33 rigid bodies);
  - braking trolley (24 rigid bodies);
  - tension rod (5 rigid bodies);
  - route rail (23 rigid bodies);
  - components of the route suspensions (268 rigid bodies).
- 13 cylindrical, 111 revolute, 298 spherical, and 15 fixed joints;
- 7 vectors of forces and torques (there are 2 driving torques; 4 braking forces, 1 braking torque);
- 18 spring—damping elements (located in the suspension system of operator's cabin, cabin for crew transportation, and in the braking trolley);
- 1172 3D items of the contact model.

The model has 720 DOF (degrees of freedom). A 3D contact model was defined between: Braking pads and route rail; rollers and route rail; and drive gears and route rail. It was defined as combination of virtual spring and damper located between solid bodies being in contact. During interaction between these two bodies, the length of virtual spring decreases, and there is some penetration of one body into the second body (in this model, the maximum value of penetration is 1×10^{-4} m). The next very important parameter of contact is contact force, which was calculated according the Formula (1) [16]:

$$F = \begin{cases} \max\left(k(x_1 - x)^e - c\dot{x},\, 0\right) & \text{at} x \le x_1 \\ 0 & \text{at} x > x_1 \end{cases}, \tag{1}$$

where:

- F—contact force;
- K—stiffness of the virtual spring;
- x_1—length of the virtual spring at the moment of the bodies contact;
- x—instantaneous length of the virtual spring;
- e—virtual spring linearity coefficient; e = 1 means a linear relationship;
- c—damping coefficient of the virtual damper;
- $\dot{x}$—relative speed of interacting bodies.

The damping coefficient "c" doesn't have constant value, which change according the Equation (2) [16]:

$$(p) = \begin{cases} 0 & \text{at } p \leq 0 \\ c_{max}\left(\frac{3}{h^2}p^2 - \frac{2}{h^3}p^3\right) & \text{at } 0 < p \leq h, \\ c_{max} & \text{at } p > h \end{cases} \quad (2)$$

where:

c—damping coefficient;

c_{max}—maximum damping coefficient;

h—penetration depth of one solid into another;

p—function describing dependence of the damping factor c on the depth of the solid penetration.

In the computational model contact parameter values were set as following:

- 3D contact between rollers and gears with the rails:
  - Virtual spring rigidity coefficient $k = 7 \times 10^9$ N/m;
  - damping coefficient $c_{max} = 7 \times 10^4$ N·s/m;
  - maximum penetration depth $h_{max} = 1 \times 10^{-4}$ m;
  - virtual spring linear coefficient e = 2.2.
- 3D contact between braking pads with the rails:
  - Virtual spring rigidity coefficient $k = 9.5 \times 10^8$ N/m;
  - damping coefficient $c_{max} = 1 \times 10^5$ N·s/m;
  - maximum penetration depth $h_{max} = 1 \times 10^{-4}$ m;
  - virtual spring linear coefficient e = 2.2.

The second part of the computational model, which is the implementation of the control system for the dynamic part of the computational model, was developed in the Matlab/Simulink environment. Then, by defining the input/output signals from each part of the computational model and by using the parallel simulation technique [17–19], numerical simulations using the developed computational model were carried out. This technique allows simulations in various software environments. In this way, it is possible to integrate various domains with each other, or to evaluate complex mechanical systems in the defined criteria states, e.g., cooperation of multi-body systems with hydraulic systems [20], thermal energy management in the mechanical systems [21], or verification of dynamic parameters of a moving vehicle in difficult land conditions [22]. The diagram of the signals flow between the various parts of the computational model is shown in Figure 5.

The simulations of the emergency braking process were carried out in accordance with the algorithm presented in Figure 5. The simulation process began with the activation of driving torque. The velocity of the suspended monorail was constantly monitored, during the simulation. After reaching the maximum value of the velocity (declared as a boundary condition), the driving torques were deactivated and the emergency braking procedure was started by activating the braking forces and torques. When the velocity of the suspended monorail was equal 0 m/s, the braking process was deactivated, and the simulation was stopped. In addition, the monorail acceleration values were recorded throughout the simulation. On their basis, it was determined whether during emergency braking there were excessive overloads affecting the operator and passengers of the transportation set.

During normal operation of the suspended monorail and in emergency situations, such as emergency braking, the operator and transported crew are affected by vibrations and dynamic overloads related to the change of the acceleration/deceleration level. The analysis of these values allows for the acquisition of appropriate knowledge in order to increase the level of comfort and safety of passengers, in particular operators who are more exposed to the occurrence of vibrations [23–27]. The results of the work related to the analysis of the impact of vibrations and dynamic overloads on the human body and the method of their minimization have been published in [28].

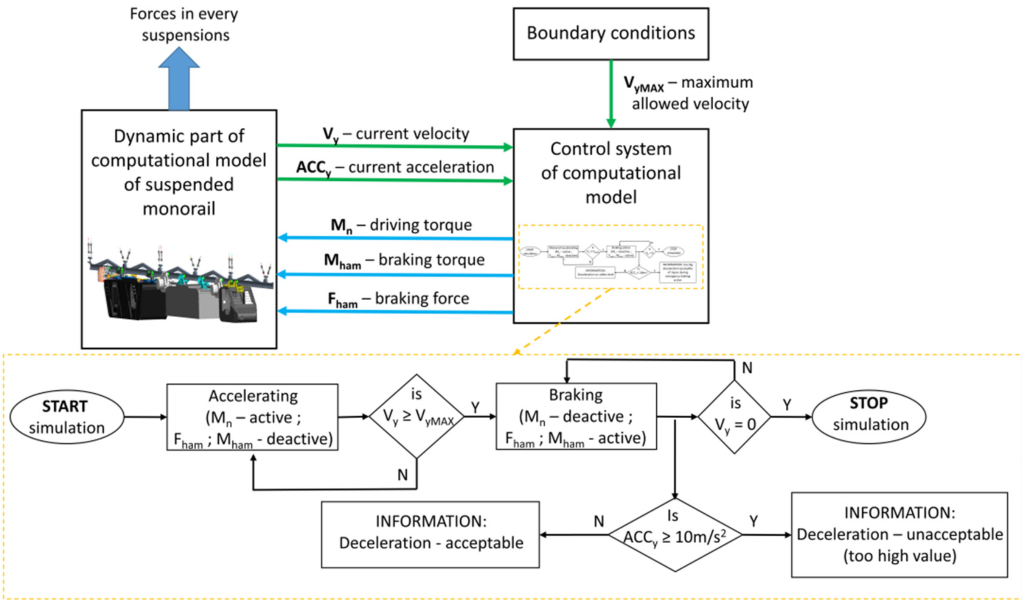

Figure 5. The structure and flow of signals in the computational model of the suspended monorail.

3. Validation of the Computational Model

Time processes of the force in the selected transducers, the forces measured during stand tests, and those calculated in numerical simulations, were compared to verify the correct operation of the computational model. Two passes were selected for comparison; first for speed 3 m/s and one for 5 m/s. For each speed, the forces were compared in one pair of vertical suspensions and one pair of diagonal suspensions. When the set was passing at a speed of 3 m/s, the forces in vertical suspensions marked with the symbol (C5 and C6) and diagonal suspensions marked with the symbol (C2 and C4) were compared. In addition, for the travel speed of 5 m/s, the forces in vertical suspensions marked (C5 and C6) and diagonal suspensions marked with symbols C8 and C9 were compared (Figure 6).

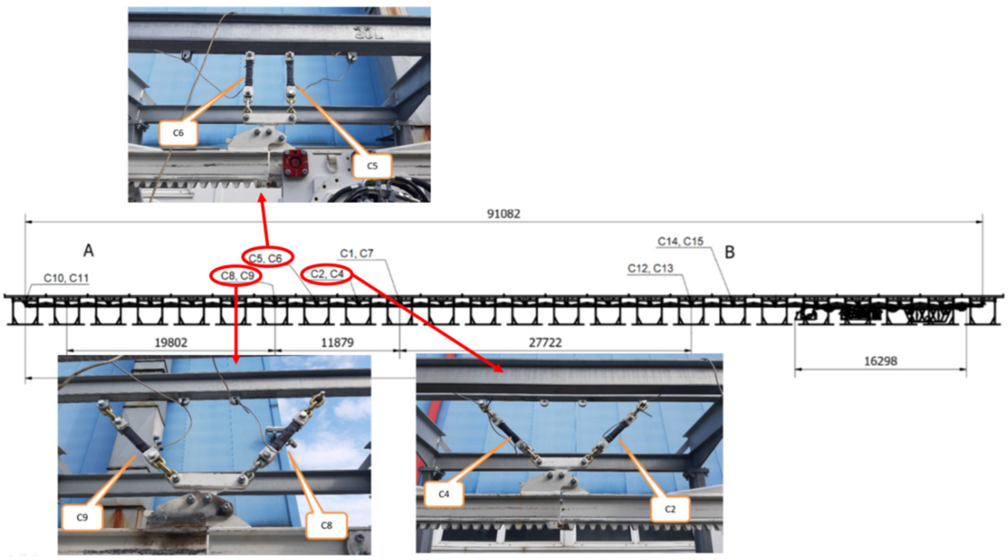

Figure 6. Arrangement of the force transducers on the measuring path: start of the ride (A), end of the ride (B)

The time curves of forces in vertical suspensions are presented in Figure 7.

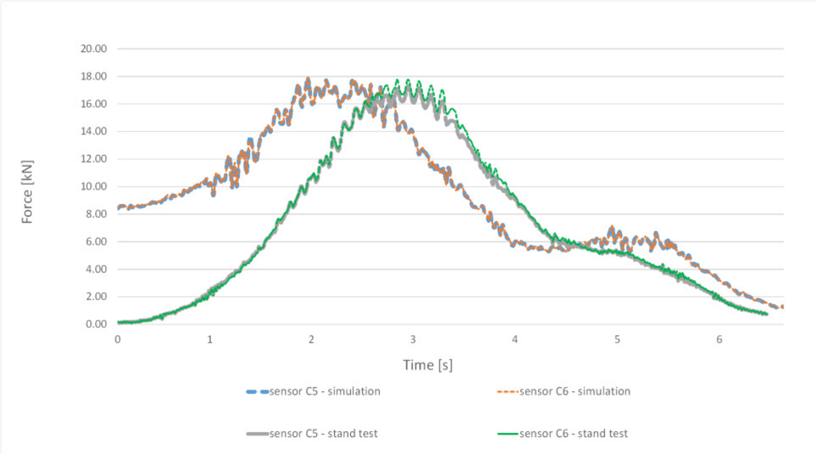

Figure 7. Force values in the vertical suspensions at travel speed 3 m/s.

Forces in the diagonal suspensions at travel speed 3 m/s are presented in Figure 8.

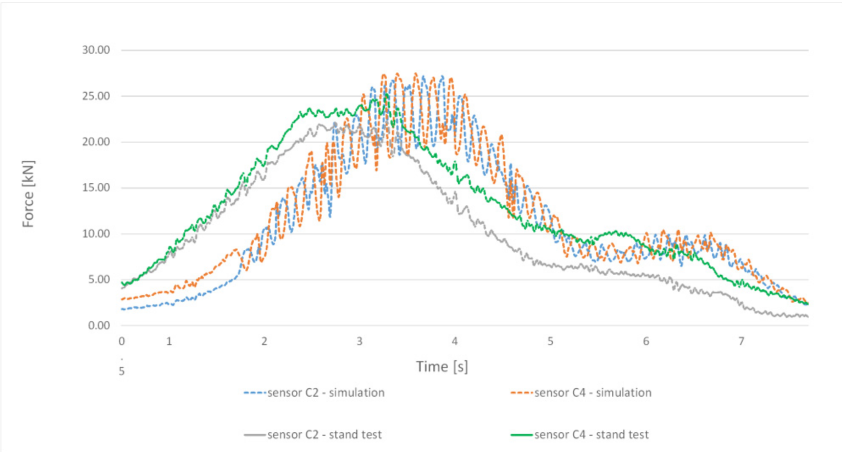

Figure 8. Force values in the diagonal suspensions at travel speed 3 m/s.

Forces in the vertical suspensions at travel speed 5 m/s are presented in Figure 9.

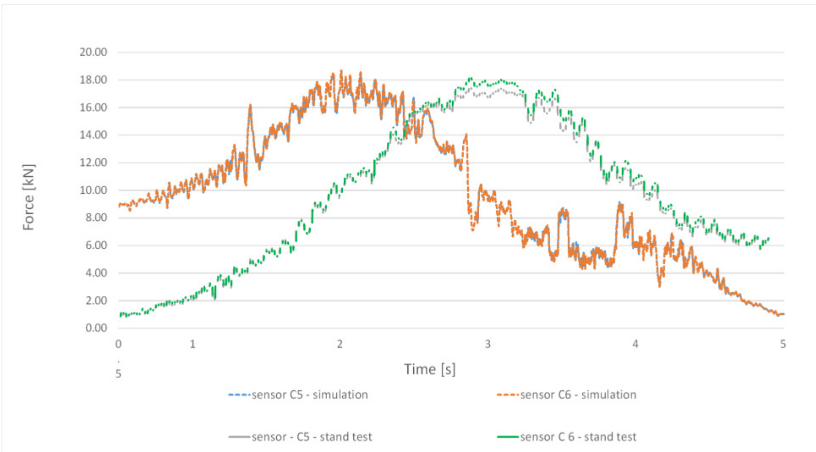

Figure 9. Force values in the vertical suspensions at travel speed 5 m/s.

Forces in the diagonal suspensions at travel speed 5 m/s are presented in Figure 10.

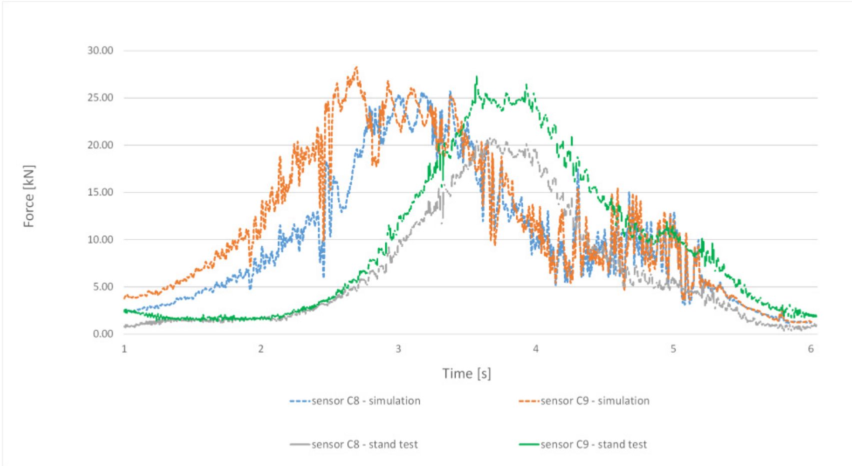

Figure 10. Force values in the diagonal suspensions at travel speed 5 m/s.

Table 1 shows the maximum forces in the selected suspensions, recorded on the test stand and calculated by numerical simulations. The percentage difference of the results obtained in the numerical calculations in relation to the values measured on the stand is also given.

Table 1. Maximum forces in each route suspension [kN].

	Calculated in Simulation [kN]	Measured on the Test Stand [kN]	Difference Calculated in Relation to the Measured Value [%]
		Travel speed 3 m/s	
Max. force in suspension C5 (vertical)	17.97	17.3	3.84
Max. force in suspension C6 (vertical)	17.93	17.78	0.87
Max. force in suspension C2 (diagonal)	27.2	22.25	22.3
Max. force in suspension C4 (diagonal)	27.49	25.27	8.79
		Travel speed 5 m/s	
Max. force in suspension C5 (vertical)	18.66	17.42	7.13
Max. force in suspension C6 (vertical)	18.71	18.14	3.18
Max. force in suspension C8 (diagonal)	25.71	20.75	23.9
Max. force in suspension C9 (diagonal)	28.27	27.29	3.57

The biggest difference was observed in the case of C8 and C2 suspensions. They are diagonal suspensions. The role of diagonal suspensions is to stabilize the suspended monorail track in the axis of travel. Depending on how the monorail is accelerated (acceleration in the speeding up phase), different forces acting on the rail are generated. As a result of these forces, the route of the monorail moves, and the role of the diagonal suspensions is to limit the range of this movement. In a situation when the suspensions chains are loosened, position of the traverse of a given rail joint can change. This results in an increase in the range of the monorail route movement, and the disproportions between the forces in a pair of diagonal suspensions increase. The described phenomenon explains large differences in the values of the maximum forces recorded on the test stand in the sensors installed diagonally

4. Analysis of the Results

After the verification of the calculation model, emergency braking of the suspended monorail assembly from the speeds equal to 1, 2, 3, 4, 5, and 6 m/s was simulated. During the simulation, the forces were recorded in each suspension of the monorail route. As only forces in the selected suspensions were measured on the test stand, in the computational model, the marking and numbering of the following suspensions were changed. Figure 11 shows the markings and numbers of each suspension along the section, where emergency braking took place.

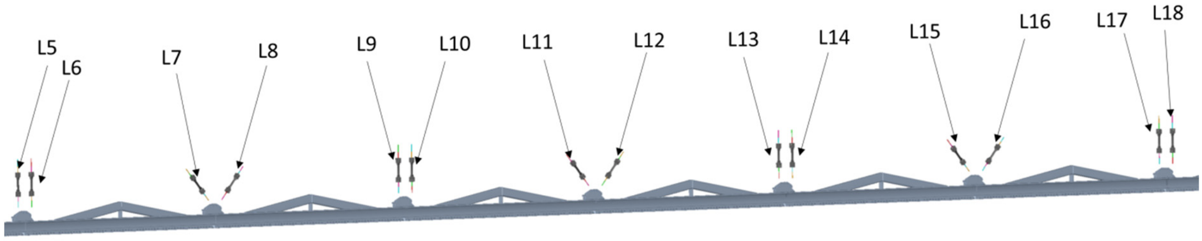

Figure 11. Marking and numbering of suspensions with force sensors in the computational model.

Moreover, emergency braking was simulated in two variants, differing in the value of the braking force. In the first simulation variant, emergency braking with full force of braking devices was used. In the second variant, the braking force was reduced by 50%.

Such an approach was aimed at emphasizing the high impact of the braking method on the forces loading the route suspensions while increasing the speed of the monorail. The maximum tensile forces in each suspension, recorded during the simulation of emergency braking at different speeds, are presented in Tables 2 and 3. In the tables, each cell is divided into two parts by a dashed line. The upper part (above the dashed line) shows the results of the simulation of braking at 50% of the braking force, while the lower part of the cell (under the dashed line) shows the values obtained in the simulations with full braking force.

Table 2. Maximum forces in suspensions recorded during simulation of emergency braking at different travel speeds (suspensions L5-L11).

Speed [m/s]/Simulation Variant		Max. Force in L12 [N]	Max. Force in L13 [N]	Max. Force in L14 [N]	Max. Force in L15 [N]	Max. Force in L16 [N]	Max. Force in L17 [N]	Max. Force in L18 [N]
1	50% F_h	3275	1181	1190	1614	1607	1282	1284
	100% F_h	3162	957	9,53	1768	1607	1282	1284
2	50% F_h	8771	1181	1190	2969	4210	1282	1284
	100% F_h	7547	972	958	2006	1607	967	955
3	50% F_h	25,058	13,981	13,988	7845	5892	1282	1284
	100% F_h	43,828	4035	4011	3752	3296	1359	1352
4	50% F_h	25,058	13,981	13,988	7845	5992	1282	1284
	100% F_h	48,407	13,887	13,950	4593	5191	1252	1228
5	50% F_h	31,728	18,272	18,176	24,138	21,749	2737	2723
	100% F_h	50,923	29,997	29,970	27,381	27,508	3403	3384
6	50% F_h	29,874	18,337	18,353	37,681	21,827	15,460	15,471
	100% F_h	32,701	16,775	16,832	55,218	32,193	17,286	17,272

* Fh—braking force.

Table 3. Maximum forces in suspensions recorded during simulation of emergency braking at different travel speeds (suspensions L12-L18).

Speed [m/s]/Simulation Variant		Max. Force in L12 [N]	Max. Force in L13 [N]	Max. Force in L14 [N]	Max. Force in L15 [N]	Max. Force in L16 [N]	Max. Force in L17 [N]	Max. Force in L18 [N]
1	50% F_h *	3275	1181	1190	1614	1607	1282	1284
	100% F_h	3162	957	953	1768	1607	1282	1284
2	50% F_h	8771	1181	1190	2969	4210	1282	1284
	100% F_h	7547	972	958	2006	1607	967	955
3	50% F_h	25,058	13,981	13,988	7845	5892	1282	1284
	100% F_h	43,828	4035	4011	3752	3296	1359	1352
4	50% F_h	25,058	13,981	13,988	7845	5992	1282	1284
	100% F_h	48,407	13,887	13,950	4593	5191	1252	1228
5	50% F_h	31,728	18,272	18,176	24,138	21,749	2737	2723
	100% F_h	50,923	29,997	29,970	27,381	27,508	3403	3384
6	50% F_h	29,874	18,337	18,353	37,681	21,827	15,460	15,471
	100% F_h	32,701	16,775	16,832	55,218	32,193	17,286	17,272

* Fh—braking force.

During emergency braking, the highest forces were recorded in the suspensions—stabilizing the position of the suspended monorail route. With the increase of the speed at which the emergency braking took place, the recorded dynamic overload in the suspensions increased. The maximum forces in the suspensions recorded for each analyzed driving speed of the set are shown in Figure 12.

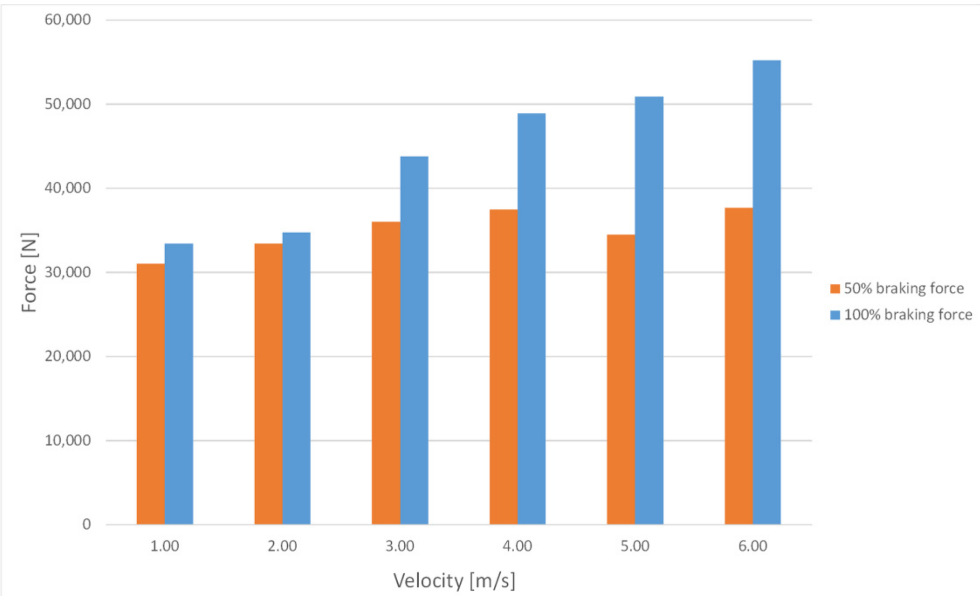

Figure 12. Maximum forces in the suspensions, in relation to maximum speeds, when braking with full and reduced braking force.

Based on the presented results, the increase in the force in the most loaded suspensions was calculated in relation to the value recorded at the lowest analyzed speed of 1 m/s

(Table 4) and in relation to the maximum speed of the suspended monorail, accepted by the legal regulations during transportation of people, i.e., 2 m/s (Table 5). The tables show the base value to which the other values were compared. The difference in forces was presented as force increase expressed in [N], and as a percentage increase in relation to the base value, both in relation to the simulation with full braking force and simulation in which the braking force was reduced by 50%.

Table 4. Increase of maximum force in the most loaded suspension in relation to the force recorded during emergency brake from the speed 1 m/s.

	Increase of the Max. Force in the Suspension When Braking 100% F_h[N]	**Percentage Increase of the Max. Force in the Suspension When Braking 100% F_h[%]**	**Increase of the Max. Force in the Suspension When Braking 50% F_h[N]**	**Percentage Increase of the Max. Force in the Suspension When Braking 50% F_h[%]**
Base value—maximum force in the suspension during emergency braking from speed 1 m/s	+33,407	-	+31,026	-
Increase of max force at speed 2 m/s in relation to 1 m/s	+1373	+4.1	+2380	+7.7
Increase of max force at speed 3 m/s in relation to 1 m/s	+10,422	+31.2	+4959	+16
Increase of max force at speed 4 m/s in relation to 1 m/s	+15,509	+46.4	+6492	+20.9
Increase of max force at speed 5 m/s in relation to 1 m/s	+17,517	+52.4	+3442	+11.1
Increase of max force at speed 2 m/s in relation to 1 m/s	+21,811	+65.2	+6654	+21.5

Table 5. Increase of maximum force in the most loaded suspension in relation to the force recorded during emergency brake from the speed 2 m/s.

	Increase of the Max. Force in the Suspension When Braking 100% F_h * [N]	**Percentage Increase of the Max. Force in the Suspension When Braking 100% F_h[%]**	**Increase of the Max. Force in the Suspension When Braking 50% F_h[N]**	**Percentage Increase of the Max. Force in the Suspension When Braking 50% F_h[%]**
Base value—maximum force in the suspension during emergency braking from speed 2 m/s	+34,780	-	+33,407	-
Increase of max force at speed 1 m/s in relation to 2 m/s	−1373	-3.9	−2380	−7.1
Increase of max force at speed 3 m/s in relation to 2 m/s	+9048	+26	+2579	+7.7
Increase of max force at speed 4 m/s in relation to 2 m/s	+14,136	+40.6	+4111	+12.3
Increase of max force at speed 5 m/s in relation to 2 m/s	+16,143	+46.4	+1061	+3.2
Increase of max force at speed 6 m/s in relation to 2 m/s	+20,438	+58.8	+4274	+12.8

* F_h—braking force.

5. Discussion

The fact that the suspended monorail route is not rigid, and both the route and the neighboring rails can change their orientation in relation to each other (possibility of movement in the rail joint) is one of the reasons for the appearance of dynamic overloads. As a result, the suspension may be momentarily loosened and then dynamically loaded.

Examples of rail displacements during emergency braking are presented in relation to rail No. 5, during braking from a speed of 5 m/s. Figure 13 shows the rail displacement along the longitudinal axis (Y axis) in line with the direction of travel of the monorail set, both in simulations with full and reduced braking force. The maximum rail displacement in this axis was 0.05 m when using the full braking force, while when using the braking force reduced by half, this displacement was 0.0141 m.

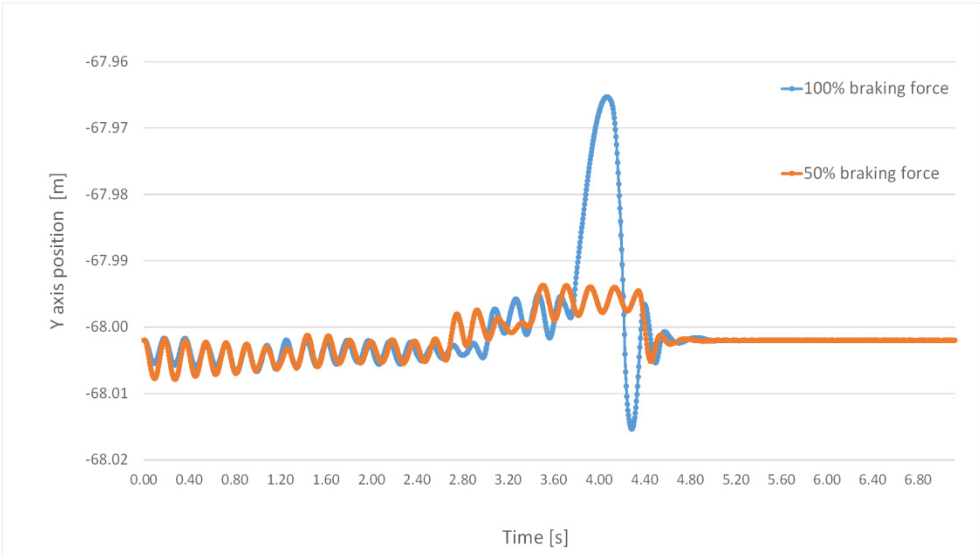

Figure 13. Displacement of the rail No. 5 along the Y axis, during braking from speed 5 m/s.

Figure 14 shows the displacement of the rail No. 5 in the vertical axis (Z axis). The maximum rail displacement in this axis was 0.0193 m when using the full braking force, while when using the braking force reduced by half, the displacement was 0.0024 m.

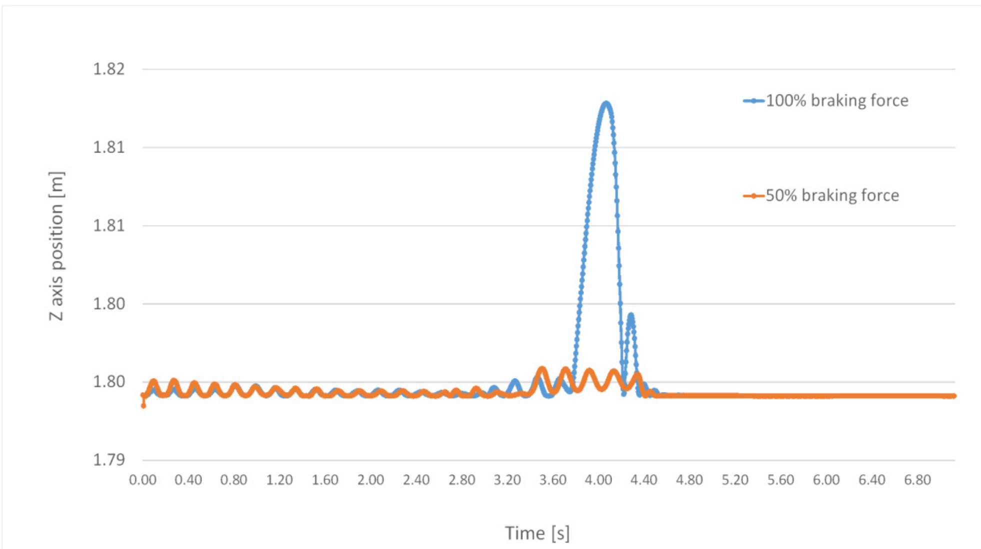

Figure 14. Displacement of the rail No. 5 along the Z axis, during braking from speed 5 m/s.

Displacement of rails changes the traverse position in suspensions, which leads to loosening of one suspension and excessive load to the other one of the pair of diagonal suspensions stabilizing the monorail route. The successive stages of changing the position of the traverse in the rail suspension and the way of loading the suspensions are shown in Figure 15.

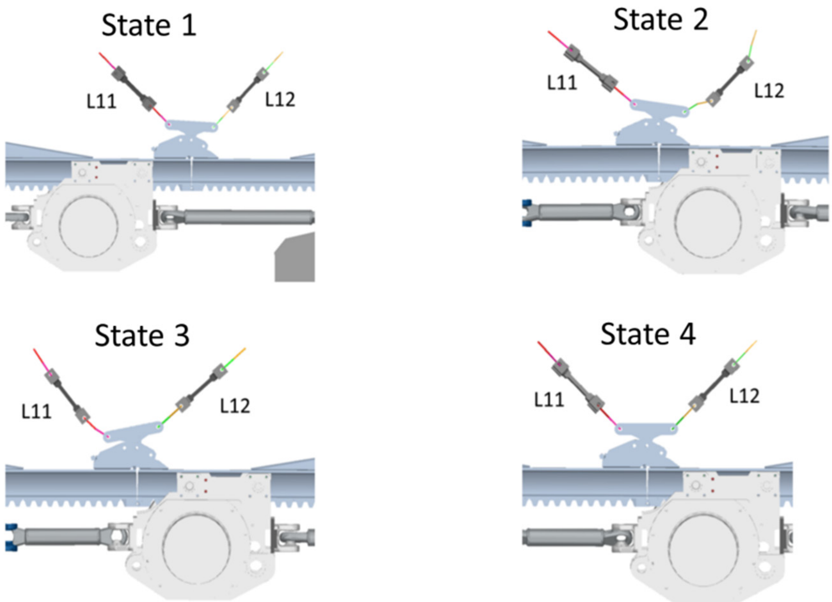

Figure 15. Successive loads to the suspensions resulting from the change of the position of the traverse in the rails suspensions.

Before braking, the suspensions are symmetrically loaded (state 1). Then, in a result of braking and action of inertia forces, the route moves forward and up—the traverse in the rail suspension rotates, and as the result, the L11 suspension is significantly more loaded (preventing against further movement of the route), and the L12 suspension is loosened and relieved (state 2). Then the track and rails return to their previous position, and the position of the traverse as a result of the action forces the suspension position changes, and the L12 suspension is dynamically hit and overloaded while loosening the L11 suspension (state 3). Stabilization and return to the balanced position and symmetrical load to the L11 and L12 suspensions is the last stage.

The analysis of the recorded forces allows us to conclude that with the increase in the maximum speed of the suspended monorail, the dynamic overloads during emergency braking with full force increase. However, reducing the braking force by half results in a significant reduction of the increase of the forces loading the route suspension. The conclusion is that along with increasing the speed of the suspended monorail, proper selection of the force and method of braking is extremely important.

6. Conclusions

The analysis shows the risk of significant dynamic overloads in the route suspensions. The diagonal suspensions stabilizing the suspended monorail's route are exposed to the greatest overload. With the increase in the maximum driving speed, the accelerations and overloads, as well as the vibrations acting on the operator and passengers of the suspended monorail also increase. These aspects were presented in other studies [29]. The simulations showed that in situations such as emergency braking, short dynamic overloads occur already when braking from the speed of 3 m/s. However, it should be mentioned that during tests a new type of rail, longer than the current one, was used (4 m long). The use of such rails improves the comfort of people travel by providing a more stable route and minimizing vibrations and overloads affecting people in the monorail, caused by improper assembly of the route. However, to distribute the weight of the suspended monorail and rails over a greater number of roof support arches, the rails require applying the special traverses at the rail joints. The analysis of the simulation results indicates that this solution may contribute to the development of dynamic overloads during emergency braking. Taking into account the aforementioned limitations and conclusions from the analyses, as well as the benefits resulting from increasing the permissible speed of the suspended monorail during the personnel movement, the authors believe that general guidelines should be developed to ensure the safe use of the monorails while increasing the permissible speed. One of the aspects concerns the way the monorail route is assembled and the selection of route sections where moving at higher speeds will be safe. This aspect includes both the appropriate selection of the route rails, the type of rail joint and the method of its suspension, and in particular the method of the used lashings stabilizing the route. It is also important to control the technical condition of the roof support arches to prevent any disturbance in its stability.

Development of an appropriate method for releasing the emergency brakes is another aspect related to minimizing dynamic overloads during emergency braking. At present, the maximum braking force is activated in a very short time, resulting in significant dynamic overloads, affecting both the route of the monorail and its suspensions, as well as people in the passenger cabins and the operator of the monorail. The authors suggest development of a special sequential method of braking, which due to the accepted increase of braking distance will reduce dynamic overloads affecting both the route suspensions and people in the monorail during braking. The use of these modifications will increase the safety of the personnel during travel.

The novelty presented in the paper are both the results of the stand tests carried out for the suspended monorail, in which the real values of the forces in the route slings while driving the transport set were obtained, as well as the conclusions obtained from the computational model. In both cases, dynamic overloads were obtained, which are crucial for the suspended route. The forces were recorded with a frequency of 150 Hz by using sensors which were specially designed and manufactured for this type of test. Due to the specificity of the suspended monorail route, dynamic overloads can be obtained in real conditions or on a specially prepared, full-size test stand. It is difficult because, in the first case, the tests are carried out in conditions of potentially explosive atmosphere, which is related to natural hazards. In the second case, in addition to the high costs of the test stand, a transportation set should be assembled. After obtaining the results from the conducted stand tests, it was possible to validate the computational model. Then, within the computer environment, the "suspended monorail research program" was extended with other variants that were not implemented on the real object.

The authors emphasize that the presented calculation results are intended to show the impact of the braking system parameters (e.g., release time, braking force, number of braking systems) on the time process of load to the suspensions of the suspended monorail's route. Modification of these parameters can significantly reduce the dynamic overload to all key components of the route, which will translate into both an increase in the level of safety for users of this type of transportation mean and extension of its service life.

Author Contributions: Investigation, K.S.; methodology, K.S.; conceptualization, K.S.; project administration, J.T.; data curation, J.T.; validation, J.T.; funding acquisition, A.W.; writing—review & editing, A.W. All authors have read and agreed to the published version of the manuscript.

Funding: This research was funded by Research Fund for Coal and Steel under grant agreement No 754169. The APC was founded by KOMAG Institute of Mining Technology.

Acknowledgments: A part of the presented work was carried out under the European project INESI, "Increase efficiency and safety improvement in underground mining transportation routes". This project has received funding from Research Fund for Coal and Steel under grant agreement No 754169. Calculations were carried out at the Academic Computer Centre in Gdańsk, Poland.

Conflicts of Interest: The authors declare no conflict of interest.

References

1. Becker, F.; Zell, M. The state of the art in positively guided rail transport systems for underground mining. *Min. Rep.* **2014**, *150*, 34–46. [CrossRef]
2. Song, Z.A.; Jiang, F. Hydraulic system elaboration and simulation for single-drive light-load monorail locomotive in fully mechanized coal mining applications. *IOP Conf. Ser. Mater. Sci. Eng.* **2019**, 474. [CrossRef]
3. Szewerda, K. Supporting development of suspended underground monorails using virtual prototyping techniques. *Mater. Sci. Eng.* **2019**, *545*, 012018. [CrossRef]
4. Małkowski, P.; Ostrowski, Ł.; Bednarek, Ł. The Effect of Selected Factors on Floor Upheaval in Roadways—In Situ Testing. *Energies* **2020**, *13*, 5686. [CrossRef]
5. Wu, G.; Chen, W.; Jia, S.; Tan, X.; Zheng, P. Deformation characteristics of a roadway in steeply inclined formations and its improved support. *Int. J. Rock Mech. Min. Sci.* **2020**, *130*, 104324. [CrossRef]
6. Li, G.; Ma, F.; Guo, J.; Zhao, H. Case Study of Roadway Deformation Failure Mechanisms: Field Investigation and Numerical Simulation. *Energies* **2021**, *14*, 1032. [CrossRef]
7. INESI European Project: Increase Efficiency and Safety Improvement in Underground Mining Transportation Routes. *RFCS*. 2017–2020, Contract No. 754169. Deliverable: D5.1: Report from laboratory tests and fields trials of transportation systems adapted to increased speed. Available online: https://www.gig.eu/en/international-projects/inesi (accessed on 8 March 2021).
8. Pytlik, A.; Rotkegel, M.; Szot, Ł. Badanie wpływu prędkości kolejek podwieszonych na siły w wybranych elementach trasy. *Przegląd Górniczy* **2016**, *11*, 30–37.
9. Zasadni, W.; Kania, J.; Tokarczyk, J.; Rusinek, J.; Szymiczek, K. Możliwości zwiększenia prędkości jazdy kolejkami podwieszonymi z napędem własnym. In Proceedings of the Problemy Bezpieczeństwa i Ochrony Zdrowia w Polskim Górnictwie, Zawiercie, Poland, 14–15 April 2015; pp. 1–10.
10. Dumitriua, M.; Gheția, M.A.; Cruceanub, I.C. Experimental Analysis of the Vertical Vibration of the Railway Bogie During Braking. *Procedia Manuf.* **2020**, *46*, 49–54. [CrossRef]
11. Gutarevych, V. Dynamic model of movement of mine suspended monorail. *Transp. Probl.* **2014**, *9*, 13–18.
12. Tokarczyk, J. *Methodology for Identifying the Selected Mechanical Hazards in Auxiliary Transport of Underground Mines, Monograph vol. 52*; Institute of Mining Technology KOMAG: Gliwice, Poland, 2018; ISBN 978-83-65593-08-5.
13. Drozd, K.; Nieoczym, A. *Dynamic Load of Suspension Chains Generated during the Movement of the Self-Powered Diesel Transportation System on a Suspended Monorail Track in the Mining Excavation*; Monograph, Lublin University of Technology: Lublin, Poland, 2020; ISBN 978-83-7947-426-4.
14. Pytlik, A. Tests of steel arch and rock bolt support resistance to static and dynamic loading induced by suspended monorail transportation. *Studia Geotech. Mech.* **2019**, *41*, 81–92. [CrossRef]
15. Horyl, P.; Šňupárek, R.; Maršálek, P.; Poruba, Z.; Pacześniowski, K. Parametric Studies of Total Load-Bearing Capacity of Steel Arch Supports. *Acta Montan. Slovaca* **2019**, *24*, 213–222.
16. Wojtyra, M.; Frączek, J. *Metoda Układów Wieloczłonowych w Dynamice Mechanizmów*; Oficyna Wydawnicza Politechniki Warszawskiej: Warsaw, Poland, 2007.
17. Verstraete, M.L.; Roccia, B.A.; Mook, D.T.; Preidikman, S. A co-simulation methodology to simulate the nonlinear aeroelastic behavior of a folding-wing concept in different flight configurations. *Nonlinear Dyn.* **2019**, *98*, 907–927. [CrossRef]
18. Spiryagin, M.; Persson, I.; Wu, Q.; Bosomworth, C.; Wolfs, P.; Cole, C. A co-simulation approach for heavy haul long distance locomotive-track simulation studies. *Veh. Syst. Dyn.* **2019**, *57*, 1363–1380. [CrossRef]
19. Jiang, Y.Z.; Zhong, W.S.; Wu, P.B.; Zeng, J.; Zhang, Y.C.; Wang, S. Prediction of wheel wear of different types of articulated monorail based on co-simulation of MATLAB and UM software. *Adv. Mech. Eng.* **2019**, *11*, 1–13. [CrossRef]
20. Rahikainen, J.; Kiani, M.; Sopanen, J.; Jalali, P.; Mikkola, A. Computationally efficient approach for simulation of multibody and hydraulic dynamics. *Mech Mach Theory* **2018**, *130*, 435–446. [CrossRef]
21. Yuan, R.; Fletcher, T.; Ahmedov, A.; Kalantzis, N.; Pezouvanis, N.; Dutta, N.; Watson, A.; Ebrahimi, K. Modelling and Co-simulation of hybrid vehicles. A thermal management perspective. *Appl. Therm. Eng.* **2020**, *180*, 115883. [CrossRef]
22. Gat, G.; Franco, Y.; Shmulevich, I. Fast dynamic modeling for off-road track vehicles. *J. Terramechanics* **2020**, *92*, 1–12. [CrossRef]
23. Desai, R.; Guha, A.; Seshu, P. Multibody Biomechanical Modelling of Human Body Response to Direct and Cross Axis Vibration. *Procedia Comput. Sci.* **2018**, *133*, 494–501. [CrossRef]
24. Lynas, D.; Burgess-Limerick, R. Whole-body vibration associated with underground coal mining equipment in Australia. *Appl. Ergon.* **2020**, *89*, 103162. [CrossRef] [PubMed]
25. Issevera, H.; Aksoy, C.; Sabuncu, H.; Karan, A. Vibration and Its Effects on the Body. *Med. Princ. Pr.* **2003**, *12*, 34–38. [CrossRef]
26. AlShabi, M.; Araydah, W.; ElShatarat, H.; Othman, M.; Younis, M.B.; Gadsden, S.A. Effect of Mechanical Vibrations on Human Body. *World J. Mech.* **2016**, *6*, 273–304. [CrossRef]
27. Kowalski, P.; Zając, J. Research on Simultaneous Impact of Hand–Arm and Whole-Body Vibration. *Int. J. Occup. Saf. Erg.* **2012**, *18:1*, 59–66. [CrossRef]
28. Szewerda, K.; Tokarczyk, J.; Bożek, P.; Michalak, D.; Drwięga, A. Vibrations diagnostics and analysis in operator's and passenger cabins of a suspended monorail. *Acta Montan. Slovaca* **2020**, *2*, 150–158.
29. Herbuś, K.; Szewerda, K.; Świder, J. Virtual prototyping of the suspended monorail in the aspect of increasing the permissible travel speed in hard coal mines. *Eksploat. Niezawodn.* **2020**, *4*, 610–619. [CrossRef]